16th World Conference on Earthquake Engineering, 16WCEE 2017
Santiago Chile, January 9th to 13th 2017
Paper N° XXXX (Abstract ID)
Registration Code: S-XXXXXXXX

VISCOUS DAMPING IN ELASTIC SEISMIC RESPONSE

D. Bernal[(1)]

[(1)] *Northeastern University, Civil and Environmental Engineering, Center for Digital Signal Processing, Boston, MA 02115, bernal@neu.edu*

Abstract

Classical damping constitutes an infinitely small subset of all possible dissipation distributions and, as such, it is never the best fit to the actual mechanism. The model is, however, widely adopted because the information needed to specify a non-classical distribution is seldom available in the design phase. From a practical perspective the question is not, therefore, whether the damping is classical or not, but whether errors attributable to adopting the classical model may be important. A result that has been known for many years but which is not widely recognized is the fact that if the poles of the dominant modes are well separated the off-diagonal terms of the damping in modal coordinates have a small effect in the response. For closely spaced frequencies, however, the specifics of the distribution are important and response predictions using the classical model can be in significant error. Needless to say, the matter takes special relevance when the ratio of effective motion duration to fundamental period is large since damping is most important in these cases. Other than recognize that uncertainties arising from the damping model are particularly large when frequencies are close, there is usually little that can be done about this matter (within practical constraints) at the design stage. This paper includes analytical work clarifying the role of the frequency gap and exemplifies the analytical observation in numerical simulations.

Another issue sometimes raised regarding the suitability of the damping model pertains to the discrepancy between the (essentially) frequency independent dissipation observed in tests and the linear dependence associated with viscosity. Could this matter be such that the identified apparent damping shows dependence on the spectral characteristics of the excitation? Although the strict answer is yes, and the paper shows this to be so in an academic example, analytical examination and numerical results show that the identified damping for realistic input motions is the one that matches the rate of dissipation at resonance. The paper also takes a look at the question of the fictitiously high damping that is sometimes attributed to the mass proportional term in the Rayleigh model when base isolation is used and shows that this "undesirable feature" does not arise if the added terms in the augmented terms of the damping are adequately formulated.

The paper includes a summary from a study where first mode damping ratios were identified for a large number of steel, concrete, masonry and wood structures and used to obtain predictive equations. It is shown that in steel and concrete the regressor with the most predictive ability is building height and it is contended that this is so because this parameter is a surrogate for the ratio of building volume to footprint, and thus to energy loss at the soil-structure interface. In masonry and wood structure the optimal regressor is shown to be the 5% damped pseudo-acceleration spectral ordinate. The limits that information theory impose on the variance with which damping can be identified from earthquake response is discussed and it is shown that for typical conditions the lower bound of the coefficient of variation is 25 to 50 times larger than for natural frequency.

Keywords: damping; identification; inelastic response; collapse

1. Introduction

The energy input from an earthquake is the work done by the forces acting at the soil-structure interface. Energy balance considerations show that this work is equal to the sum of the kinetic and the strain energies plus the running integral of the work of the non-conservative forces. In practice it is customary to separate the non-conservative work into the work done by hysteresis in the structural system plus the work of a collection of unspecified mechanisms that are aggregated an referred to as "the damping". This aggregate is not generally viscous but viscosity, i.e. damping forces proportional to velocity, is commonly assumed on grounds of mathematical convenience. This paper reviews the formulation of the equivalent viscous model and presents a summary of results obtained in a study where first mode damping ratios were identified from measured data in a large number of buildings.

2. The Classical and Non-Classical Damping Viscous Model

Accepting equivalent viscosity and finite dimensionality the damping model, either explicitly or implicitly, consists of a damping matrix, $C \in R^{nxn}$, where n is the number of degrees of freedom in the model. Specifying the damping matrix as classical is tantamount to stating that C is diagonalized by a congruent transformation using the un-damped mode shape matrix Φ, namely, that

$$\Phi^T C \Phi = \begin{bmatrix} 2\omega_1\xi_1 & & & \\ & 2\omega_2\xi_2 & & \\ & & . & \\ & & & 2\omega_n\xi_n \end{bmatrix} \tag{1}$$

where ω_j *and* ξ_j are the un-damped frequency and damping ratio of the j[th] mode. A necessary and sufficient condition for the damping to be classical is that the eigenvectors of $M^{-1}K$ and $M^{-1}C$ coincide. Since matrices with common eigenvectors commute the necessary and sufficient condition for a damping matrix to be classical is that $M^{-1}K$ and $M^{-1}C$ commute. It is a simple matter to show that any classical damping matrix can be written in terms of the mass normalized mode shapes as

$$C = M\left(\sum_{j=1}^{n} \gamma_j \phi_j \phi_j^T\right) M \tag{2}$$

where $\gamma_j = 2\omega_j\xi_j$. An alternative expression that does not require computation of the mode shapes, known as the Caughey series [1,2] is

$$C = M\sum_b a_b \left(M^{-1}K\right)^b \tag{3}$$

where b are integers. It can easily be shown that the coefficients a_b are related to the damping ratios by

$$\xi_j = \frac{1}{2\omega_j}\sum_b a_b \omega_j^{2b} \tag{4}$$

A widely used special form, known as Raleigh or proportional, writes

$$C = \alpha M + \beta K \tag{5}$$

where α and β are constants. It is a simple matter to show that the damping ratios in this model vary with frequency according to the expression

$$\xi_j = \frac{1}{2\omega_j}\left(\alpha + \beta\omega_j^2\right) \tag{6}$$

which can be used to compute the $\{\alpha, \beta\}$ constants by specifying the damping ratio at any two frequencies.

A Weighted Least Square Alternative

Although damping ratios can be easily prescribed at all desired frequencies using Eq.2, the Rayleigh model is popular in earthquake engineering and discussion on which two modes to select have appeared through the years: first and second, first and last, etc.; the objective being to keep the damping close to the desired target in the "important modes" while ensuring that the damping of other modes do not distort the results. Here we note that instead of selecting which modes to target, explicitly, the target damping can be specified at all frequencies of interest and the constants solved in a weighted least square sense. The solution is

$$\begin{Bmatrix}\alpha\\ \beta\end{Bmatrix} = \left(Q^T W^T W Q\right)^{-1} Q^T W^T L \tag{7}$$

with

$$Q = \begin{bmatrix}1 & \omega_a^2\\ 1 & \omega_b^2\\ \vdots & \vdots\\ 1 & \omega_q^2\end{bmatrix} \quad \text{and} \quad L = 2\begin{Bmatrix}\omega_a\xi_a\\ \omega_b\xi_b\\ \vdots\\ \omega_q\xi_q\end{Bmatrix} \tag{8a,b}$$

where W is the weighting matrix, which can be taken as $W = diag(\omega_a^{-v} \quad \omega_b^{-v} \quad \cdots \quad \omega_q^{-v})$ with the exponent v controlling how the difference between the target damping ratio and the value realized is affected by frequency. For v = 0 one gets the standard least square solution, which, due to the form of L, is dominated by the high frequencies, v = 1 leads to residuals that are independent of frequency and for v>1 the lower frequencies are more heavily weighted.

2.1 Base Isolation

Consider a structure for which the damping matrix has been assembled on a fixed base condition and one is interested in examining what happens to the damping ratios when a soft spring is added at the base. The isolation will, of course, also add a localized damping contribution but the present discussion can be carried out neglecting this added damping. The argument made in [3] is that the damping of the first mode in the isolated case, which should be very small because the mode shape approximates rigid body motion, becomes unreasonably large if the initial damping matrix has a mass proportional contribution. While this is the case if the added partitions are taken as zero, it is not so if the damping matrix of the originally fixed base model is expanded as Eq.9 indicates. Namely, designating the fixed base matrix as C_f it follows from equilibrium considerations that the enlarged matrix after the isolation is added is

$$C_I = \begin{bmatrix}C_f & -C_f r\\ (-C_f r)^T & r^T C_f r\end{bmatrix} \tag{9}$$

where r = pseudo static displacement vector, which in the 2D model typically used to discuss buildings is a sequence of ones for horizontal input. Inspection of Eq.9 shows that the dissipation is zero for rigid body motion and, as can be seen, this result is independent of the form of C_f. We take the opportunity to note that the mass proportional damping contribution vanishes (from the Rayleigh model) if the damping is assembled in the unrestrained condition and the rigid body modes are assigned zero dissipation.

2.1 Non-Classical Damping

Classical damping matrices are isolated points in parameter space and as such the probability that the dissipation is best described by a classical distribution is zero. The model is ubiquitous, however, since it can be economically specified, namely, it requires only *n* damping ratios and, with the possible exception of systems with small eigenvalue gaps, it can provide a good approximation to the dissipation. To analytically illustrate the relative unimportance of deviations from classical when poles are not too close we examine a 2-DOF system with an arbitrary non-classical viscous dissipation. Transferring the equations of motion to the coordinates of the undamped modes and accepting all the usual assumptions one gets

$$\begin{Bmatrix} \ddot{Y}_1 \\ \ddot{Y}_2 \end{Bmatrix} + \begin{bmatrix} 2\omega_1\xi_1 & \tau \\ \tau & 2\omega_2\xi_2 \end{bmatrix} \begin{Bmatrix} \dot{Y}_1 \\ \dot{Y}_2 \end{Bmatrix} + \begin{bmatrix} \omega_1^2 & \\ & \omega_2^2 \end{bmatrix} \begin{Bmatrix} Y_1 \\ Y_2 \end{Bmatrix} = \begin{Bmatrix} -\phi_1^T Mr \\ -\phi_2^T Mr \end{Bmatrix} \ddot{x}_g \tag{10}$$

where $\tau = \phi_1^T C \phi_2$ and where it's evident that we've assumed the modes to be mass normalized. With j,k ={1,2} or j,k={2,1} one has

$$\ddot{Y}_j + 2\omega_j \xi_j \dot{Y}_j + \omega_j^2 Y_j = -\phi_j^T Mr \cdot \ddot{x}_g - \tau \dot{Y}_k \tag{11}$$

Taking a Fourier transform of Eq.11 and solving for the modal amplitude gives

$$Y_j(\omega) = \frac{-\phi_j^T Mr \ddot{x}_g(\omega) - \tau\omega Y_k(\omega)}{(\omega_j^2 - \omega^2) + 2\omega_j\omega\xi_j i} = \frac{a_j - \tau\omega Y_k(\omega)}{d_j(\omega)} \tag{12}$$

which, after some simple rearrangement can be written as

$$\left(1 - \frac{(\tau\omega)^2}{d_1 d_2}\right) Y_j(\omega) = \frac{a_j}{d_j} - \frac{\tau\omega a_k}{d_1 d_2} \tag{13}$$

In the classical model $\tau = 0$ and the modal response (in frequency) is the first term on the *rhs* of Eq.13. Error from deviations from classical depend, therefore, on how large is the (absolute value) of the second term in the *lhs* parenthesis, compared to one, and on how large the second term in the *rhs* is compared to the first. The term in the parenthesis is

$$\frac{(\tau\omega)^2}{d_1 d_2} = \frac{\left(\frac{\tau}{\omega}\right)^2}{\left((\beta_1^2 - 1) + 2\beta_1\xi_1 i\right)\left((\beta_2^2 - 1) + 2\beta_2\xi_2 i\right)} \tag{14}$$

where $\beta_j = \omega_j / \omega$. This ratio takes its largest values when the numerator is large and the denominator small. Accepting that the damping ratios are small it is reasonable to inspect the expression at resonance, for $\beta_1 = 1$ one has

$$\frac{(\tau\omega)^2}{d_1 d_2} = \frac{\left(\frac{\tau}{\omega_1}\right)^2}{\left(-4\beta_2\xi_1\xi_2 + 2\xi_1(\beta_2^2 - 1)i\right)} \cong \frac{\left(\frac{\tau}{\omega_1}\right)^2 i}{2(1 - \beta_2^2)\xi_1} \tag{15}$$

Accepting an upper bound on τ of 50% of the first entry in the diagonal of the C matrix in Eq.10, and taking $\xi_1 = \xi_2 = \xi$ one has

$$\left|\frac{(\tau\omega)^2}{d_1 d_2}\right| \le \left|\frac{\xi}{2(1-\beta^2)}\right| \tag{16}$$

where we've eliminated the subscript from β. Since we used the first frequency to arrive at Eq.16 it follows that $\beta > 1$. As can be seen from Fig.1, the ratio examined is small relative to one, except in cases where the frequency of the second mode is close to the first. Specifically, for 2% and 5% damping the bound is less than 0.1 for $\beta > 1.04$ and 1.12, respectively.

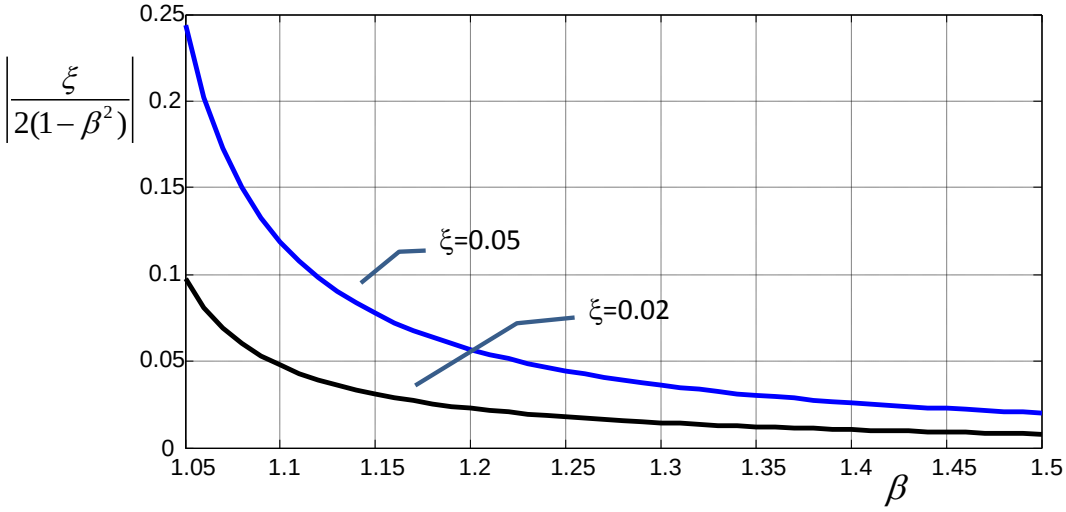

Fig.1 (Quasi) upper bound of Eq.16 vs the ratio of undamped frequencies.

Examination of the importance of the second term in Eq.13 compared to the first can be carried out in the same fashion as before, namely, taking the ratio of the second term to the first, assuming that a_1 and a_2 are equal, that the damping ratios are small, and taking the bound on τ as stated previously one gets that this ratio is

$$\frac{\xi}{(\beta^2 - 1)} \tag{17}$$

which is simply twice the value plotted in Fig.1; the term is no larger than 0.1 if $\beta > 1.1$ and 1.25 for 2% and 5% damping respectively. It's opportune to note that the closeness of the frequencies as the critical factor in the relevance of the deviations of damping from classical was pointed out early on by Rayleigh [4], who showed that the first order approximation of the complex mode shape, z_j, is given by

$$z_j \approx x_j + i\sum_{\substack{k=1 \\ k\neq j}}^{j} \frac{\omega_j C_{kj}}{(\omega_j^2 - \omega_k^2)} x_k \tag{18}$$

where x_j is the real mode shape and C_{kj} are the off-diagonal coefficients of the damping matrix in the undamped modal coordinates .

Numerical Illustration

We test the previous assertions using a 2-DOF system in two different configurations, one where the frequencies are very close and the other where they are reasonably separated. To better isolate the effect of the frequency gap the parameters are chosen so that the difference between the actual damping matrix and the approximation given by the classical model has the same norm in both instances. The system, initially considered in [5] is depicted in

Fig.2a: when $\theta_k = \theta_c = 1$ there is a nearly repeated pole at $-0.073 \pm 1.50i$ and in the configuration, $\theta_k = 2, \theta_c = 1.55$ the undamped frequencies are 1.46 and 2.17 rad/sec. Responses for both configurations are obtained for the SCT record of the Mexico City earthquake of 1985 and the repeated pole configuration is also driven by a signal recorded at the base of CSMIP station 13214 during the ChinoHills earthquake. The SCT record is narrow band with duration for the central 90% of the Arias intensity of around 41 secs while ChinoHills is wide band and has duration of around 24 secs.

Figs2b-d depict the response at coordinate #2 computed with the exact damping and with the classic approximation obtained by neglecting the off-diagonal terms in the modal basis. In the case of the repeated pole and the SCT record the results, which are shown in (b) show there is an underestimation of the positive peak of around 45%, which is significant. For the configuration with the separated frequencies in (c) the max error is, however, only 13%. Finally, as shown in (d) for the case of the repeated pole, the large error of Fig.2b virtually vanishes when the ChinoHills record is used because the peak response occurs on the first pulse and is thus little affected by damping.

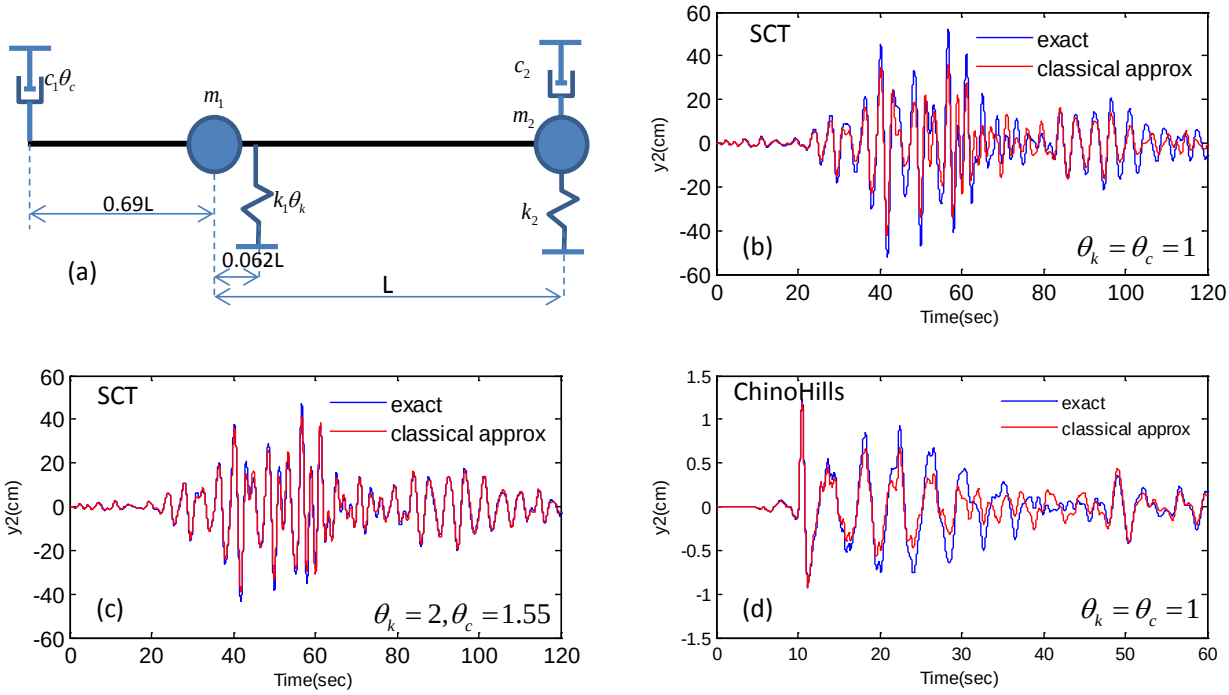

Fig.2 a) System considered (m_1=1, m_2=2, k_1=2.68θ_k , k_2 =4.29, c_1 =0.078θ_c , c_2 = 0.102), b-d) displacement response at mass #2.

2.2 Damping Ratio

The rate of decay of the homogeneous response of a SDOF system (or of a complex mode in phase space) is determined by the real part of the pole and the frequency of vibration by the imaginary. The pole λ is typically written as

$$\lambda = -\omega\xi \pm i \cdot \omega\sqrt{1-\xi^2} \tag{19}$$

from where it follows that

$$\xi = \frac{-\lambda_R}{|\lambda|} \tag{20}$$

It is important to keep in mind that ω in Eq.19 coincides with the un-damped natural frequency ONLY when the damping distribution is classical. To clarify consider a 2-DOF shear building with m={1,1} k={50,50} c={a,0}. The smallest value of the dashpot constant "a" for which one of the system poles is purely real is a = 17.678 and for this case one finds, from Eq.20, that the "damping ratios" are {0.25,1}. Assume now that one reduces "a" to "0.05a". Since the damping matrix has uniformly decreased to 5% of the original, one may expect that the damping ratios would be 5% of the previous ones, namely {0.0125, 0.05} but what is obtained, however, is {0.028, 0.028}. The interpretation of damping ratio as a fraction of the minimum level required to suppress harmonic terms in the homogeneous solution applies only when the damping is classical, otherwise the meaning is simply that it is the value given by Eq.20.

3. Hysteretic Damping

The energy dissipated per cycle in a SDOF system with viscous damping that executes harmonic motion is proportional to the frequency and to the square of the amplitude. Experimental evidence shows that the square amplitude dependence is closely realized but dependency on frequency is typically small. The idealized mathematical model where dissipation is frequency independent is known as hysteretic. The relation between the damping force and the response in the hysteretic model is

$$f_D(t) = -\frac{\eta}{\pi}\int_{-\infty}^{\infty}\frac{u(\tau)}{t-\tau}d\tau \tag{21}$$

where η is a constant. Recognizing that the Hilbert transform of the function f(t) is defined by

$$H(f_{(t)}) = \frac{1}{\pi}\cdot\int_{-\infty}^{\infty}\frac{f(\tau)}{t-\tau}d\tau \tag{22}$$

one has

$$f_{D(t)} = -\eta\cdot H(u(t)) \tag{23}$$

Fundamental examination shows that the viscous and the hysteretic models dissipate the same energy under harmonic motion if

$$\eta = c\Omega \tag{24}$$

where Ω is the imposed motion frequency. Although the hysteretic model can be implemented without difficulty in the frequency domain, in the time domain, as would be needed to perform nonlinear analysis, the model is cumbersome because (as Eq.21 shows) the damping force is in this case non-causal, i.e., the force at time *t* depends not only on the displacement past, but also on its future.

3.1 Frequency Content of the Motion

Although strict frequency independence violates causality and cannot, therefore, be the exact mathematical form of the dissipating mechanism, the hysteretic model is often a reasonable approximation and for the purpose of this section we take it as valid. On this premise, and since the hysteretic and viscous models can only be made equivalent at a single frequency, a reasonable question is whether the frequency content of the excitation may play a role on the (equivalent) damping that is identified from data. If the damping is hysteretic and the excitation is harmonic at frequency Ω the viscous damping with the same dissipation rate

is $\xi = 0.5(\eta/k)(\omega/\Omega)$. From theory, therefore the answer appears to be yes, and to test it we consider two excitations: A =broad band (white noise) and B = (very) narrow band obtained by passing the white noise signal through a bandpass filter that retains components only in the vicinity of 11π (rad/sec). We compute the response of SDOF system with $\omega_0 = 2\pi$ and hysteretic damping given by $\eta/k = 0.1$ and use the simulation results to identify the equivalent damping using a subspace algorithm [6]. For motion B the pure harmonic based prediction is $\xi = 0.5(0.1)(2\pi/11\pi) = 0.009 \cong 0.9\%$ and what the identification algorithm gave is 0.8%, which is quite close. For the A motion the expectation is that the identified damping will correspond to equivalence at resonance, i.e. to 5% and what was obtained was 4.96% - confirming the expectation.

The previous result validates the theoretical argument but is rather contrived because the motion considered is "unreasonably narrow band". A study using the SCT record from the 1985 Mexico City earthquake, which is a strongly narrow band, real motion, showed that the identified damping was in all cases the value that, at resonance, matched the hysteretic dissipation. The conclusion appears to be, therefore, that real records are not sufficiently close to pure sinusoids to make the issue of damping dependence on the input spectrum one of practical relevance.

4. Accuracy Limits on Damping Estimation

Discussion of identified damping values in the literature are often confused because the results are interpreted as "real" and not as estimates under noise subject to limitations on variance error imposed by information theory. To illustrate qualitatively why the variance on identified damping is high let there be a region around the true (albeit unknown) pole where, given the noise, the identification algorithm places the pole. Assume the region of uncertainty is a circle of radius *R*, where *R* is a fraction of the pole magnitude, say $R = \beta|\lambda|$ where β is small (e.g., 0.02). To determine if the circular assumption is reasonable we performed Monte Carlo simulations with a 6-DOF system identified for a given ground motion using 1000 different random realizations of the noise. As can be seen in Fig.3, which shows the results for the first and the second pole, the circular premise is not unreasonable. Examination of the geometry shows that the estimated frequencies, for the large majority of the data, will be in the interval $\omega[(1-\beta) \quad (1+\beta)]$, while the damping ratios fall in the interval $[(\xi-\beta) \quad (\xi+\beta)]$. If β is 0.02, for example, the frequency error is no more than 2% but the damping ratio can be over or under estimated by 0.02. Namely, if the true damping is 5% one can easily get values as large as 7% and as low as 3%.

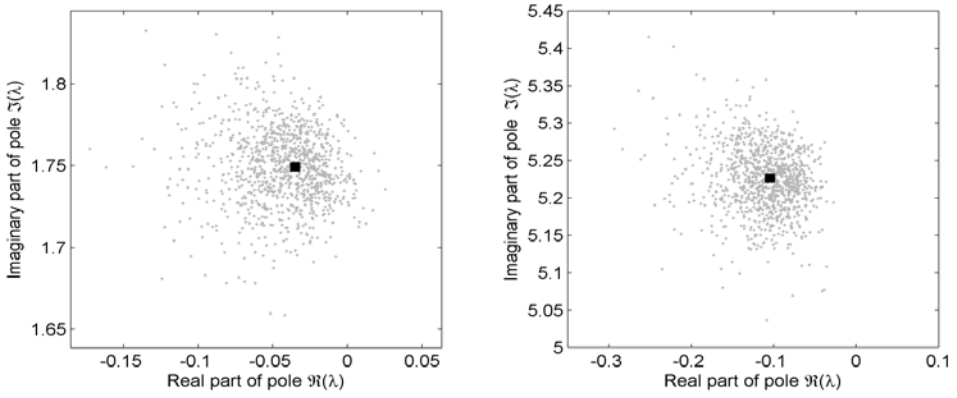

Fig.3 Real and imaginary parts of the 1st and 2nd pole in a 6-DOF system identified using white excitation and 5% additive noise.

4.1 Fisher Information and the Crámer-Rao Lower Bound

It is instructive to derive an expression for the theoretical limit of the ratio of the coefficient of variation of identified damping to identified frequency. For any distribution of the noise affecting the input and the output the information on a set of parameters, θ, is quantified by the Fisher Information (FI) matrix, $I(\theta)$ and the lower bound of the covariance Σ of any estimator of these parameters is given by its inverse, known as the *Cramér-Rao Lower Bound* (CRLB) [7]. The Fisher information matrix and, as a consequence, the CRLB, depend only on the statistical distribution of the noise and on the sensitivity of the data to the parameter but not on the estimator. The FI can be defined in terms of the gradient or the Hessian of the probability distribution with respect to the parameters as

$$I(\theta) = \mathbf{E}\left(\frac{\partial}{\partial \theta} \log f(Y \mid \theta) \right)^2 \tag{26}$$

where $f(Y \mid \theta)$ is the likelihood function of the observed data Y given the parameter θ. If the sensitivity of the likelihood to the parameter is high the derivative in Eq.26 is large and so is $I(\theta)$. In practice the likelihood function $f(Y \mid \theta)$ is in general unknown so other quantities derived from the data are typically used to estimate $I(\theta)$. For example, if the data Y can be used to generate a vector X whose distribution is a member of the linear exponential family having a mean $\gamma(\theta)$ and a covariance Σ then the FI of the parameter θ contained in X can be obtained as [8]

$$I(\theta) = \mathrm{J}\ (\theta)^T \Sigma^{-1} \mathrm{J}\ (\theta) \quad \text{where} \quad \mathrm{J}\ (\theta) = \frac{\partial \gamma}{\partial \theta} \tag{27}$$

To illustrate the significance of Eq.27 in a simple setting let the "true" value of Y be deterministically dependent on θ as depicted schematically in Fig.4 Assume one wants to know the value of θ based on noisy values of Y. From the sketch in the figure it is evident that the statistical accuracy of θ depends on the slope of the functional relation at the location of the estimate and it is not difficult to see that the variances are related by the square of the local slope. Eq.27 is the generalization of this concept to the multivariate situation.

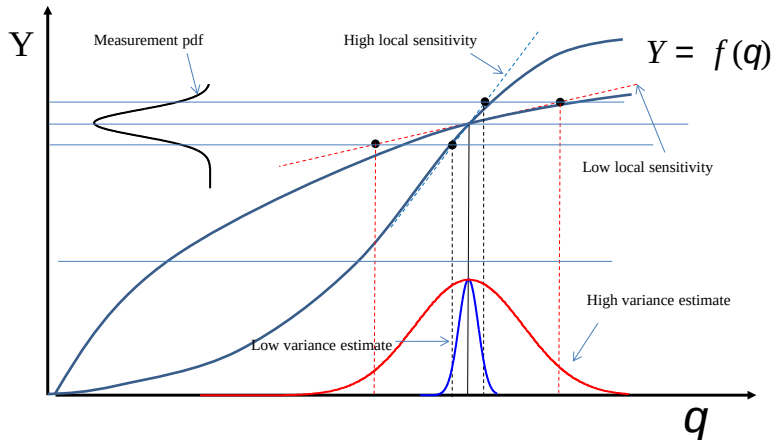

Fig.4 Schematic illustration of Eq.23 in the scalar case.

The Pole as a Feature

Denoting Σ_λ as the CRLB of the real and imaginary parts $\Re(\lambda)$ and $\Im(\lambda)$ of a pole λ, the FI of the frequency and the damping follows from Eq.27 as

$$I(\xi, f) = \mathrm{J}_{\xi,f}^{T} \Sigma_\lambda^{-1} \mathrm{J}_{\xi,f} \tag{28}$$

where the sensitivity of the pole with respect to damping ratio and frequency is given by

$$\mathbf{J}_{\xi,f} = \frac{\partial(\Re(\lambda),\Im(\lambda))}{\partial(\xi,f)} = 2\pi\begin{bmatrix} -f & -\xi \\ -f\xi(1-\xi^2)^{-\frac{1}{2}} & \sqrt{1-\xi^2} \end{bmatrix} \tag{29}$$

Assuming that the uncertainty region around the complex poles is circular the ratios between the COVs are shown in Fig.5. As can be seen, the uncertainty on the damping ratios is around 50 times higher than that for the frequencies at $\xi = 2\%$, and the ratio is near 25 for $\xi = 5\%$. These results are consistent with the findings in [9], where maximum likelihood estimation of modal parameters from ARMA models was considered.

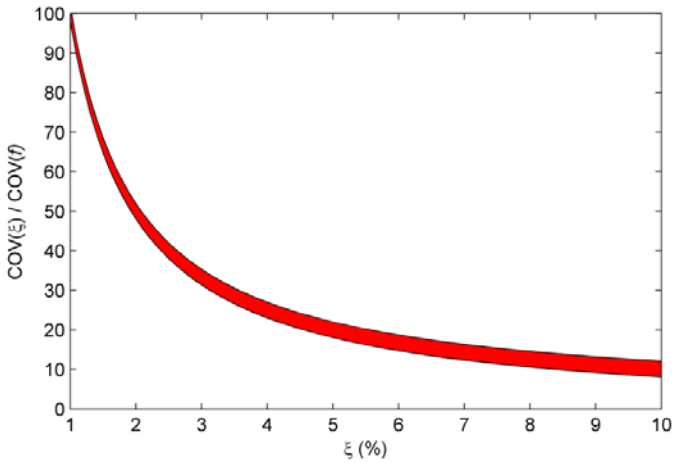

Fig.5 Range of the ratio of the coefficient of variation of damping and frequency when the uncertainty region around the pole is circular.

5. Regression Analysis on Real Building Data

It has been traditional to specify damping ratios as 2 % for steel and 5 % for concrete. Efforts to determine expressions that reduce the variance associated with this practice have been carried out in the past few decades. Here we review recent results obtained in a study whose details are summarized in [10]. With ϑ as the regressors and θ as the vector of model parameters one has, in general

$$\xi \approx g(\theta,\vartheta) \tag{30}$$

where ξ are damping ratios estimated from data. The functional relationship g is not suggested by theory in the case of damping so it must be selected from inspection of the data. The regressors considered in [10] were: the peak ground motion parameters (PGA, PGV and PGD), the spectral ordinates (SA, SV and SD), the building height, H, the modal frequency, *f*, and the effective duration $t_{0.9}$. This last entry defined as the time interval between the attainment of 5 and 95 % of the total integral of the acceleration squared [11]. Not included due to lack of information, but potentially important, are parameters related to the soil and the foundation and to the type and density of partitions. Building material is not a parameter in the regression because the buildings were pre-classified by material type. The parameters θ are obtained by minimizing a norm of the discrepancy between the model predictions and the data. Selecting the square of the two-norm of the residual as the objective function, J, one has

$$J = \left\| \omega_i \cdot \left(g(\theta,\vartheta_i) - \xi_i \right) \right\|_2^2 \tag{27}$$

where ω_i are weights. Ideally the weights should be taken as inversely proportional to the standard deviation of the estimates and in this regard it is shown in [10] that this deviation can be taken as

$$\sigma_{\xi} = \frac{\kappa}{\sqrt{f \cdot t_{0.9}}} \tag{28}$$

where κ is a constant that is immaterial in the optimization. Two functional forms were selected: one for cases where the damping decreases and the other for when the damping increases with the regressor. With the parameters as $\theta = \{a_0, a_1, a_2\}$ or $\{b_0, b_1, b_2\}$ and the regressors as ϑ these are

$$\xi = a_0 + a_1 e^{-a_2 \vartheta} \tag{29}$$

$$\xi = \frac{b_0}{1 + b_1 e^{-b_2 \vartheta}} \tag{30}$$

The regression was carried out for identified first mode damping ratios of 122 cases of concrete buildings, 81 steel, 26 masonry and 10 wood. The cases were selected from the CSMIP database as those for which the ground acceleration was no less 5% of gravity and the intensity was such that significant inelastic behavior could be ruled out. The regressor that led to the smallest variance for steel and concrete buildings proved to be the building height, H, and for masonry and wood the 5% damped spectral acceleration at the first mode period. With the height in meters and the spectral acceleration in g's the best fit expressions at expectation are;

$$\xi = 1.2 + 4.26 e^{-0.013H} \quad (steel) \tag{31a}$$

$$\xi = 3.01 + 3.45 e^{-0.019H} \quad (concrete) \tag{31b}$$

$$\xi = \frac{1}{0.11 + 0.23 e^{-8.84 S_A}} \quad (masonry) \tag{31c}$$

$$\xi = \frac{1}{0.09 + 0.17 e^{-3.37 S_A}} \quad (wood) \tag{31d}$$

with a standard deviation on the expectation model for steel and concrete of approximately 0.8% . It is believed that the reason why the height proved the best regressor in the steel and concrete buildings (for which the range of heights was significant) is because this variable is a good surrogate for dissipation at the soil-structure interface, i.e. as buildings gets taller the ratio of the footprint to the building volume decreases and the interface dissipation decreases. Note that the foregoing is not an argument about SSI, which speaks about differences between fixed base and compliant foundations, but rather between "fixed base" and "floating", the latter being a situation where the apparent damping would be smaller than the values we measure.

Discussion

For steel buildings the height provided the best correlation with damping ratio by a significant margin while for concrete buildings the expression based on S_A was only slightly poorer. For masonry and wood buildings the correlation with S_A was clearly the superior choice and this matches what one expects from qualitative reasoning. Examinations not shown here due to space constraints but which can be found in [10] show that dependence on S_A saturates very quickly in steel and less so in concrete. A question that comes to mind is whether a multivariate regression using both H and S_A would lead to notable improvements in the predictive formulas. This was tried and the answer proved negative because the correlation between these two parameters is significant. Indeed, as the height increases the period lengthens and the spectral accelerations, except for short buildings, decrease.

6. Closing Commentary

The traditional argument for the Rayleigh model is expediency, namely, the fact that the model is specified by only two parameters. This argument, however, has lost much of its strength since coding of arbitrary classical damping is not, at present, a significant computational burden, even for models with thousands of DOF. Another argument often mentioned is that arbitrary classical damping leads to a full matrix, which does not reflect the "actual connectivity". This argument is also less than compelling since connectivity is not a physical reality but a model property (divide every element in two and the "connectivity changes"). The paper shows that the classical model, albeit never realized, is a reasonable simplification because the distribution details do not have an important effect in the response, except when there are closely spaced poles. In cases where the system has closely spaced frequencies (in the relevant bandwidth) there is usually little that can be practically done, other than to keep in mind that the uncertainties in predictions are larger than when the frequencies are well separated. The paper shows that the variance with which damping can be identified from earthquake response is much larger than that of frequency and that, as a consequence, the variability often observed in instrumented structures is not intrinsic but reflects this high variance. The expressions for the first mode damping ratio presented in the paper were obtained from a relatively large ensemble and are believed to provide some reduction in variance over the 2% and 5% damping traditionally used for steel and concrete structures.

7. Acknowledgment

The expressions for first mode damping ratios presented were developed during work supported by the California Strong Motion Instrumentation Program through standard agreement 1010-934. Some additional support for work on the general subject of damping in earthquake engineering was also provided by NEES Grant 1134997. This support is gratefully acknowledged.

8. References

[1] Caughey TK (1960): Classical normal modes in damped linear systems. *J Appl Mech* 27(2), 269– 271

[2] Caughey TK, O'Kelly MEJ (1965): Classical normal modes in damped linear dynamic systems. *J Appl Mech* 32(3), 583–588

[3] Hall J.F., (2006): Problems encountered from the use (or misuse) of Rayleigh damping, *Earthquake Engng Struct. Dyn*. 35, 525–545

[4] Rayleigh, Lord (1877): Theory of Sound (two volumes), Dover Publications, New York, reissued 1945, second edition.

[5] Bernal, D. (2005): Closely spaced roots and defectiveness in second order systems, *J. Eng. Mech.* 131,(3), 276-281

[6] Di Ruscio, D. (1996): Combined deterministic and stochastic system identification and realization: DSR: a subspace approach based on observations. Modeling, Identification and Control, 17(3), 193-230.

[7] Casella, G. and Berger, R. (2001): Statistical Inference, Duxbury Press.

[8] van den Bos A (2007): Parameter estimation for scientists and engineers. Wiley Interscience

[9] Gersch, W. (1974): On the achievable accuracy of structural system parameter estimates, Journal of Sound and Vibration 34(1), 63–79.

[10] Bernal D, Döhler M, Kojidi SM, Kwan K, Liu Y (2013): First mode damping ratios, *Earthquake Spectra*, 31,(1), 367-381.

[11] Arias A. (1970): Measure of Earthquake Intensity, *Seismic Design for Nuclear Power Plants*, Hansen, Robert J. (ed.). Cambridge, MIT Press, 438-83.